Journal of Hydraulic Structures
***J. Hydraul. Struct.*, 2018; 4(2):60-80**
DOI: 10.22055/jhs.2018.27833.1092

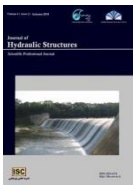

OPEN ACCESS

Evaluating performance of meta-heuristic algorithms and decision tree models in simulating water level variations of dams' piezometers

Rezvan Salajegheh[1]
Amin Mahdavi-Meymand[2]
Mohammad Zounemat-Kermani[3]

Abstract

Monitoring the seepage, particularly the piezometric water level in the dams, is of special importance in hydraulic engineering. In the present study, piezometric water levels in three observation piezometers at the left bank of Jiroft Dam structure (located in Kerman province, Iran) were simulated using soft computing techniques and then compared using the measured data. For this purpose, the input data, including inflow, evaporation, reservoir water level, sluice gate outflow, outflow, dam total outflow, and piezometric water level, were used. Modeling was performed using multiple linear regression method as well as soft computing methods including regression decision tree, classification decision tree, and three types of artificial neural networks (with Levenberg-Marquardt, particle swarm optimization, PSO, and harmony search learning algorithms, HS). The results of the present study indicated no absolute superiority for any of the methods over others. For the first piezometer the ANN-PSO indicates better performance (correlation coefficient, R=0.990). For the second piezometer ANN-PSO shows better results with R=0.945. For the third piezometers MLR with R=0.945 and ANN-HS with R=0.949 indicate better performance than other methods. Furthermore, Mann-Whitney statistical analysis at confidence levels of 95% and 99% indicated no significant difference in terms of the performance of the applied models used in this study.

Keywords: Data driven models; dam surveillance; soft computing, heuristic algorithms, dam engineering.

Received: 8 December 2018; Accepted: 26 December 2018

1. Introduction

Seepage is one of the major issues in various engineering levees and dams, so that in most of

[1] Department of Civil Engineering, Baft Branch, Islamic Azad University, Baft, Iran.
[2] Department of Water Engineering, Shahid Bahonar University of Kerman, Kerman, Iran
[3] Department of Water Engineering, Shahid Bahonar University of Kerman, Kerman, Iran. Email address: zounemat@uk.ac.ir, orcid.org/0000-0002-1421-8671. (**Corresponding author**)

the cases, the problems related to these structures are associated, either directly or indirectly, with seepage; therefore, monitoring and identifying the seepage behavior play important role in the safety and security of the engineering levees and dams [1-3]. Piezometric devices installed and used in certain sections of the dam to measure the seepage based on water level. In relation to monitoring and investigating the issue of seepage, numerous studies have been conducted to date, most of which have been focused on investigating the seepage rate and seepage monitoring in different sections of dams [4]. Although concrete dams are considered impenetrable, they have been encountering serious seepage-related problems due to their specific construction conditions [2]. In practice, in order to monitor seepage, some piezometers are improvised in certain parts of the dam [5, 6].

In addition, some other physical methods (drilling boreholes and using dye trace test) as well mathematical models and numerical methods can be also used to identify the seepage path and solve the seepage path problems [7].

In recent decades, regarding the successful application of data-based methods for simulating various kinds of engineering problems, the soft computing methods have been widely used for solving the dam engineering problems. Several studies have evaluated the performance of these methods in predicting the dam location variation, dam section optimization, and fracture in arch dams [1].

In order to predict water level in piezometers, Tayfur et al. [8] used ANN, and considered the upstream and downstream water levels as the input data. Gholizadeh and Seyedpoor [9] used neural network and PSO (particle swarm optimization) and GA (genetic algorithm) to show the impact and importance of soft computing in achieving the optimal arch dam design geometry, which can provide stability of the dam against natural pressures.

Zhou et al. [5] used a compound method, consisted of orthogonal design (OD), ANN, FE, and GA, for modelling the leakage and seepage problems. Zhou et al. [5] used BPNN (back-propagation neural network) to depict the implicit map of environmental parameters in order to investigate the impermanent seepage flow's response at dam monitoring points. Stojanovic et al. [10] presented a self-tuning system for dam behavior modelling based on ANN with genetic algorithm (ANN/GA) compared to MLR, the results of which implied superiority of the ANN-GA method over other methods. Xiang et al. [4] used PSO algorithm to optimize the seepage model parameters, the results of which indicated the higher precision and accuracy of this method compared to previous statistical methods.

Nourani et al. [11] used neural network and ANFIS (adaptive network-based fuzzy interference system) to investigate contamination concentration over time in porous environments. Studies have shown that the complexity of the underground water flow and transmission of contamination have caused the use of black box methods, such as neural networks and ANFIS.

The present study is aimed to simulate the water level in piezometers of Jiroft double-curvature arch dam in Kerman province, Iran, using three samples of MLP artificial neural networks (with Levenberg-Marquardt training algorithm as well as PSO and HS algorithms), and to compare the results obtained from the MLR, classification decision tree, and regression decision tree methods. To best of the authors' knowledge, assessing the performance of classification regression tree, regression decision tree, ANN-PSO and ANN-HS to predicting the water level in piezometers has not been studied in past researches. Hence, the application of these soft computing models is the novelty and the contribution of this study.

.

2. Materials and methods

2.1. Case study and dataset

Jiroft dam is a double-curvature arch concrete dam operated in 1991, which is located in the study zone of Hamun-e-Jaz Murian at the central basin and is fed by Halilriver in the northeast of the Jiroft city in the narrow valley of Narab (Figure 1). This dam has been constructed with the aim of generating electricity and supplying the water requirement of agricultural and environmental sectors; besides, it is also used as a secondary target for supplying drinking water. The electricity generation capacity of this dam is 80 GW, and it features reservoir volume of 336 m^3, dam height of 128 m, height above its foundation of 132 m, crest length of 250 m, and lake length of 12 km; also, the spillway is of middle and surface sluice type [12].

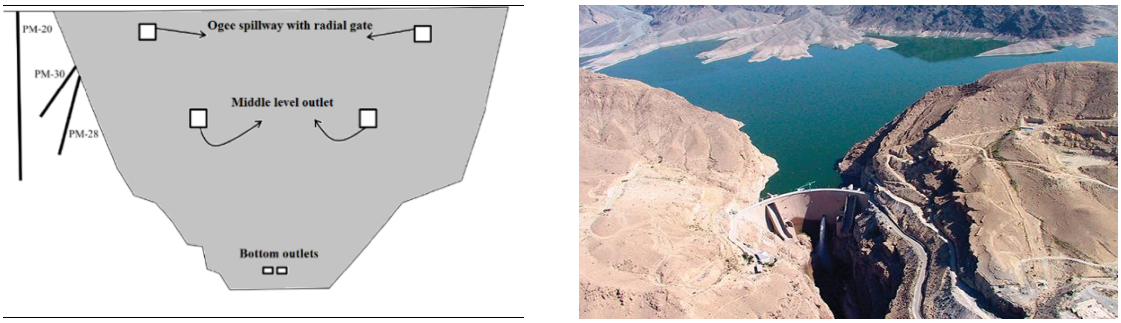

(a) **(b)**

Figure 1. (a) Aerial image of Jiroft double-curvature arch concrete dam in Kerman province, Iran; (b) Schematic image of cross section of dam and location of piezometers used in this study, which are situated at left bank retain wall in the body and rock (rock is the foundation) of the dam.

Jiroft dam has about 22 and 19 piezometers in the right and left banks, respectively. We could access to the data of three of these piezometers (see Figure 1). So, in order to model the water level behavior caused by seepage in Jiroft concrete dam, the data related to the piezometers 20, 28, and 30 situated at the left bank retain wall was used. Piezometer 20 is located at the abutment (support), and piezometers 28 and 30 are situated in the dam body. The obtained data on the water level of the piezometers were used as the output parameter of each model. The water level in these piezometers was measured once a month since 1994 to 2001; also, the input vector of each model was developed based on the monthly data, including evaporation rate from water surface (mm), reservoir inflow (m3/s), reservoir water level (m), sluice gate outflow rate (MCM), Intake outflow (MCM), as well as total outflow rates (MCM) in the given period. It should be noted that the reservoir inflow and evaporation rates were taken from the nearest station to the dam site (Kenrouye Station) at a 12km distance. The number of datasets for each piezometer is 192.

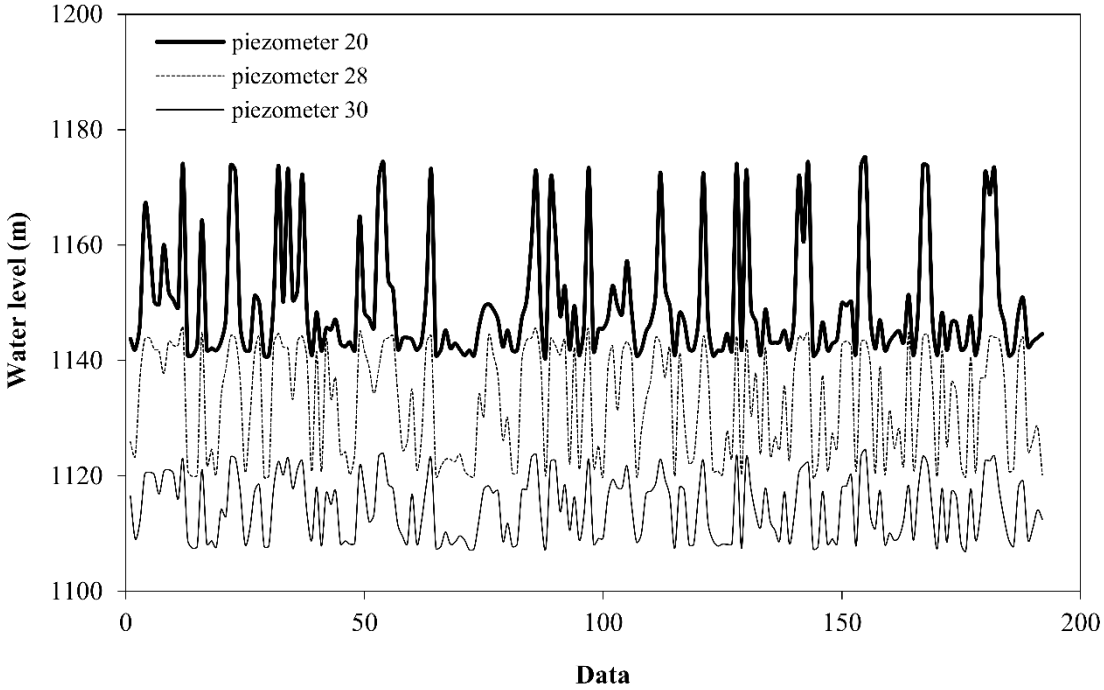

Figure 2. Historical variations of water level in the three studied piezometers in this research.

Figure 2 shows the historical variations of water level in the three piezometers. As could be expected from the location of piezometers (see Figure 1), the average values of surface water level in Piezometer 20 is more than the other two piezometers. Also total variations in Piezometer 28 is less than the other two piezometers. In this study the hold-out method is used as the method of sampling. In this respect, datasets are divided into two categories of training (80%) and testing (20%) phases for modelling implementation. Training data are used for the learning process of the models, while testing data are used to evaluate the performance of the models. A summary of the statistical characteristics of the measurement data of the output vector (reservoir water level variations) and input vector is provided in Tables (1) and (2).

Table 1- Statistical analysis of piezometers' water level data used in the present study

Piezometer	Max (m)	Min (m)	Ave (m)	SD	CV	SK
20	1175.1	1140.9	1149.657	10.235	0.008	1.472
28	1145.55	1119.84	1132.954	9.442	0.00	-0.150
30	1124.48	1107.07	1114.459	5.473	0.004	0.175

Table 2 - Statistical analysis of input parameters of data driven models

Parameter	Max	Min	Ave	SD	CV	SK
Input discharge to the reservoir (m3/s)	150.769	0.038	8.111	17.871	2.203	4.500
Evaporation (mm)	541	54.5	264.480	136.429	0.515	0.175
Water level of the reservoir (m)	1183.52	1120.99	1153.845	17.669	0.015	0.216
Sluice gate outflow rate (MCM)	110.75	0	5.222	20.520	3.929	4.457
Intake outflow(MCM)	28.94	0	6.180	5.219	0.844	1.420
Total outflow rate(MCM)	461.498	0.942	24.255	49.598	2.044	6.268

2.2 Data driven models used in this study

2.2.1 MLR model

Multiple (multivariate) linear regression is a method in which two or more independent variables contribute to the variations of a variable, and is one of the most effective prediction methods; thus, it is widely used in researches that are aimed to investigate and predict a specific phenomenon. In such researches, regarding the independent variables, a regression relation is extracted, based on which the dependent variable is predicted. The general form of the equation is as follows [1, 10]:

$$WL = \beta_0 + \beta_1 u_1 + \beta_2 u_2 + \ldots \beta_N u_N \quad (1)$$

where, WL stands for the piezometer's water level (dependent parameter) and β_i represents coefficients of the independent parameters and is estimated by sum of square error, and u_i indicates the input variable vector [13].

2.2.3 Decision tree models

A decision tree represents a structure in which the leaves indicate classes (categories), and the branches indicate combinations of the attributes resulting in these classes. Decision trees classify the samples by sorting them in the tree from the root toward leaf nodes. Each internal node in the tree tests an attribute of the sample, and each branch coming out of that node corresponds to a possible value for that attribute. Each leaf node represents a class. Each sample begins from the root and after testing the attribute in this node, moves in the corresponding branch with regard to the attribute, and finally is placed in an appropriate class. This process is repeated regressively for each sub tree. The regression is completed when further separation is not useful anymore or a classification cannot be applied to all the samples existing in the obtained subset [14, 15].

Decision trees are capable to generate attributes from the relations in a dataset, which are perceivable for human and can be used for classification and prediction. Decision trees are divided into four main groups, including classification trees, regression trees, classification-regression trees, and cluster trees. In the present study, two types of these trees, namely classification and regression trees are used [15-17].

2.2.3.1 Regression decision tree (RDT)

Regression decision trees were first introduced by Breiman et al. [14] as a statistical model. These trees are based on the regression divisions of the training data in groups of similar cases.

The output of a medium decision tree is the observed output variable in each group. When there is more than one predictor, the best separator (distinction) point is calculated for each of them, and the factor resulting in the highest error reduction rate is selected; therefore, the inappropriate (irrelevant) predictors are automatically eliminated by the algorithm, so that error reduction for a separator in a low-importance predictor will be generally less than that in a more useful one. Other dominant characteristics of the regression decision trees include [17] : they are robust against outliers, require little data preprocessing, can handle numerical and categorical predictors, and are appropriate for modelling nonlinear relations, as well as interaction among predictors.

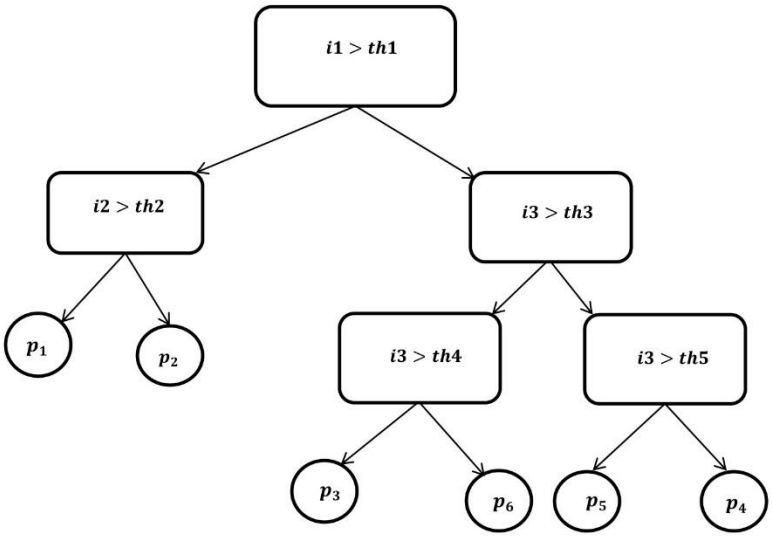

Figure 3. Schema of structure of a regression decision tree

Figure 3 shows a profile of a regression decision tree [15] . In order to improve precision of prediction, it calculates the re-substitution error, test sample error, and cross-validation error. The error is estimated by applying the data used for determining the structure of the predictor p and is calculated as the MSE (mean square error).

$$\mathrm{E}(\mathrm{p})=\frac{1}{\mathrm{N}}\sum_{\mathrm{i}=1}^{\mathrm{N}}\left(\mathrm{u_i}-\mathrm{p}\left(\mathrm{v_i}\right)\right)^2 \tag{2}$$

Where, (ui, vi) indicates training samples, and i=1,2,3,…,N is divided into K subsamples in order to estimate the re-substitution error of sample X with size of N. Also, $X_1,X_2,\ldots,X_K$ with approximate size of $N_1,N_2,\ldots N_K$ from $X\text{-}X_K$ subsamples are used for making the predictor p. Finally, this error of the sample X_K is calculated using the following formula:

$$E^{cv}\left(P\right)=\frac{1}{N_k}\sum_{k}\sum_{(u_i v_i)\in x_k}\left(v_i-p^{(k)}\left(u_i\right)\right)^2 \tag{3}$$

Where, ($p^k u_i$) is calculated from the subsample $x\text{-}x_k$. The test sample error is divided into subsamples x_1 and x_2 with size of N_1 and N_2, and then is calculated using the following formula:

$$E^{ts}(p)=\frac{1}{N_2}\sum_{(u_i v_i)\in X_2}^{N}\left(v_i-p_{ui}\right)^2 \tag{4}$$

where, x2 is a subsample that is not used in the prediction structure.

Finally, the output of each decision tree is calculated via the following formula:

$$R(t)=\frac{1}{N_w(t)}\sum_{i\in t} w_i f_i\left(u_i-\bar{v}(t)\right)^2 \tag{5}$$

Where, $N_w(t)$ is the weight of data at t, w_i is the value of the weighting variable for case i, f_i is the value of the frequency variable, v_i is the value of the response variable, and $\bar{v}(t)$ is the weighted mean for node t.

2.2.3.2 Classification decision tree (CDT)

Classification decision trees are used to predict discrete data (Figure 4). In order to have a better classification tree, the classification process must have error freedom as much as possible. This means that final nodes of the tree should be as homogenous as possible regarding the predicted variable. For this purpose, a step-wise algorithm creates an optimal classification of the training data, in which both categorical and prediction variables are known and clear. At each step, all of the possible branches are tested and compared based on each explanatory variable. And finally, the selected branch introduces the optimal subset [16, 18, 19].

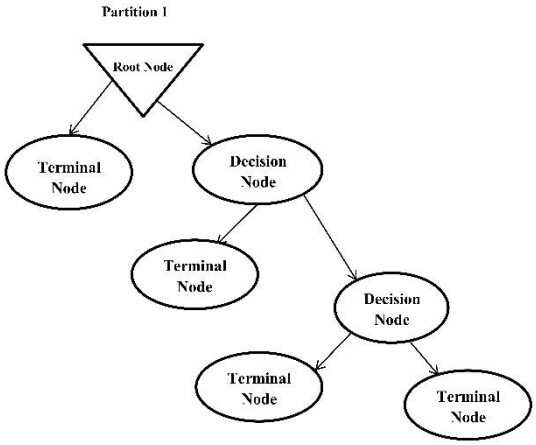

Figure 4. Schema of a classification decision tree

Since various indices and methods have been proposed so far for determining the decision tree, accordingly various algorithms have been introduced as well, the most important of which is CART (classification and regression tree) algorithm that has been designed for quantitative variables, but meanwhile it can be used for any type of variable. This algorithm was first introduced by Breiman et al. [14]. In this algorithm, various indices are used as criteria for selecting the variables. One of these indices is the Gini Index (GI), the advantage of which over other indices is its higher computation speed. In the present study, the CART algorithm and GI were used for classifying and predicting the water level in piezometers [19].

$$GINI_{split} = \sum_{i=1}^{2} \frac{N_i}{\mathrm{N}} GINI_i \tag{6}$$

$$GINI_i = \sum_{j=1}^{k} \left(1 - p_j^2\right) \tag{7}$$

Where, $GINI_i$ is the GINI index of the child node i, N_i is the number of samples at the child node i, N is the number of samples at the parent node, P_j is the probability of class j at node i, and k is the number of classes.

2.2.3 Artificial neural networks (ANNs)

ANNs, with considerable ignorance, can be called the electronic models of the human brain's neural structure. In fact, the aim of creating a software neural network is, rather than simulating the human brain, to create a mechanism for solving the engineering problems inspired by the behavioral pattern of biological networks. These networks are capable to distinguish between the input patterns; thus, they can be used in a wide range of complex problems, including recognition of patterns, nonlinear models, classifications, etc. ANNs are divided into two main groups, namely recurrent networks, in which the loop occurs, and feed-forward neural networks, the structure of which lacks loops. Selecting the network's structure depends on the learning algorithm used for training of the network. A specific type of neural networks, known as FNN 3-layer neural network, has been widely used for solving many of the civil engineering and water engineering problems[1 , 20].

2.2.3.1 Back propagation feed forward neural network

There are various types of neural networks, the most important of which is the back propagation feed forward neural networks (BPFNN). Similar to other types of neural network, FNNs are composed of simple components, which are called neurons. Neurons are located in layers, and neurons of the adjacent layers are interconnected to each other via connectors of an independent unit (synapses), which transfer the information from one neuron to other ones. The input data are stored in neurons of the first layer (input layer), and the outputs are displayed by neurons of the last layer (output layer). All the layer located between the input and output layers are known as the hidden layers (Honric, 1991).

The activation function is associated with layers, and its role is to scale and classify the output data of the layers. The most common types of activation functions include linear and sigmoid types. The linear activation functions are represented by the following general form:

$$f\left(y\right) = y \tag{8}$$

Two common types of sigmoid activation functions, which are used in these networks, include hyperbolic tangent function and logistic function.

$$f\left(0\right) = \frac{1}{1+e^{-y}} \tag{9}$$

$$f\left(y\right) = \frac{1-e^{-y}}{1+e^{y}} \tag{10}$$

The output of a neuron in the hidden layers can be such as the following pattern:

Output = $f(y)$ (11)

Where $y = \sum_{i=1}^{k} w_i x_i + b$, $x_1,x_2,\ldots,x_k$ are the input signals, $w_1,w_2,\ldots,w_k$ are the neurons' weights and b is the bias component. Figure (5) shows an FNN with 3 layers and S neurons in the input layer. The inputs are $x=(x_1,x_2,\ldots x_k)$, which are collected at the hidden nodes along with weights. At the nodes, first, the signal is collected and then a nonlinear function is applied (e.g. hyperbolic tangent); finally, the output y appears under a linear function at the output nodes.

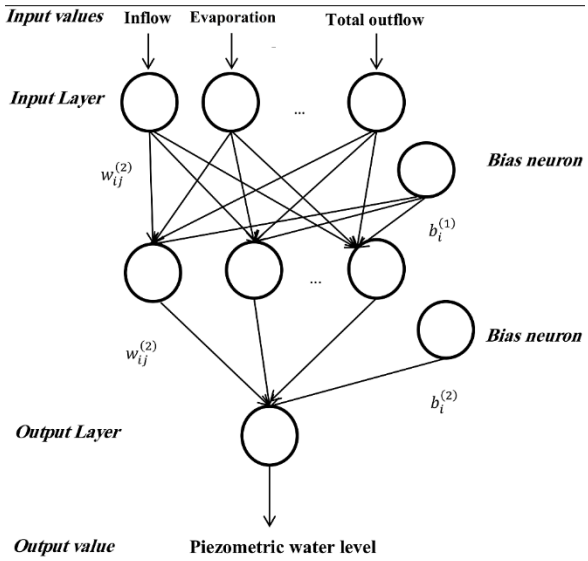

Figure 5. Three-layer neural network used in the present study

$$y = \sum_{i=1}^{k} w_{ij}^{(2)} \frac{1}{1+e^{-(\sum_{j=1}^{s} x_i w_{ij}^{(1)} + b_i^{(1)})}} + b_i^{(2)} \quad (12)$$

where, s is the number of inputs, k is the number of hidden neurons, x_j indicates j input elements, $w_{ij}^{(1)}$ is the weight of the first layers between i hidden neurons and j inputs, $w_{ij}^{(2)}$ is the weight of the second layer between i hidden neurons and the output neuron, $b_i^{(1)}$ is the base weight for i hidden neurons, and $b_i^{(2)}$ is the base weight for the output neurons [1,21].

2.2.4 Optimization methods

Optimization is indeed a method for utilizing the linear and nonlinear capability of the formulas in order to solve a wide range of problems and analyze the solutions [22]. In the present study, in order to optimize the weight values of the neurons of the ANN, the Levenberg-Marquardt mathematical optimization method as well as PSO and HS meta-heuristic optimization methods was used.

2.2.4.1 Levenberg-Marquardt mathematical algorithm

Levenberg-Marquardt algorithm is a method to find the minimum of a multivariate nonlinear

function, which is used as a standard method for solving the least square problem for nonlinear functions. It is widely used in FNNs in order for reducing the errors by point reduction of the error curve's slope [23-25].

Due to its effective role in accurate calculation of the weights' error, this algorithm has been considered and investigated as the most well-known and prominent training structure, and is currently used for generalizing the delta role (variations) in nonlinear activation functions and multi-layer networks. In Marquardt algorithm, the error function is minimized, while the size of the computational steps is small; accordingly, in order to reassure accuracy of the linear approximations, this objective was accomplished by the following modified error function [22].

$$E = \frac{1}{2}\left(e_{(j)} + \frac{\partial_{ek}}{\partial_{wi}}\left(w_{(j+1)} - w_{(j)} \right) \right)^2 + \lambda \left(w_{(j+1)} - w_{(j)} \right)^2 \quad (13)$$

Where, λ is the parameter representing the step size, the minimum error, with regard to $w_{(j+1)}$ is expressed as following:

$$W_{(j+1)} = W_{(j)} - \left(Z^T Z + \lambda I \right) Z^T e_j \quad (14)$$

High values of λ cause declination of the standard gradient, and its lower value inclines toward Newton method.

2.2.4.2 PSO algorithm

PSO algorithm was created by Kennedy & Eberhart [26] based on the collective movement of birds or a group of fish. PSO is an optimization sample capable to model the human population for processing the science, which is rooted in two main components of methodology, namely artificial life (such as groups of birds, schools of fish) and evolutionary counting (evolutionary computations). PSO algorithm is based on the assumption of the potential of movement in a space full of high-speed particles toward the optimal solution. It is a populated search method for optimizing the nonlinear functions [27] Furthermore, PSO extracts the best cooperation status, and uses it for optimizing the engineering problems. The particles simply follow the set of predetermined roles. PSO calculates the particles based on the performance capability, and then selects the particle with the best solution. The particle with best capability is selected as the trainer; subsequently, all the particles are trained by the selected particles. No two particles are similar, and instead they utilize other particles' attributes to improve their own performance [28].

For each particle, two values of position and speed is defined, which are modeled by a location vector and a speed vector, respectively. These particles move repeatedly in the n-dimensional space of the problem. Dimensions of the problem are determined by the number of parameters of the problems. The general form of the algorithm's equation is represented below [29]:

$$v_{ij}\left(t'+1\right) = wv_{ij}\left(t'\right) + c_1\gamma_1\left(p_{ij}\left(t'\right) - x_{ij}\left(t'\right)\right) + c_2\gamma_2\left(p_{gi}\left(t'\right) - x_{ij}\left(t'\right)\right) \quad (15)$$

$$x_{ij}\left(t'+1\right) = x_{ij}\left(t'\right) + v_{ij}\left(t'+1\right) \quad (16)$$

Where j is the number of dimensions, i is the number of particles, t' is the number of repetitions, w is the inertia weight, γ_1 and γ_1 are random numbers in the range of [0,1], c_1 and c_2 are constant acceleration in the range of [0,2], and v_{ij} is usually limited to a certain range.

$v_{ij} \in [-v_{max}.v_{max}]$, and if the search space is limited to $[-x_{max}.x_{max}]$, then $v_{max} = kx_{max}$ with $0.1 \leq k \leq 1$. Also, $p_{ij}(t) - x_{ij}(t)$ represents the distance between the current location and optimal location of the i[th] particle, and $p_{ij}(t) - x_{ij}(t)$ indicates the distance between the current location and the optimal location of the i[th] particle in the group.

2.2.4.3 HS (harmony search) algorithm

Harmony search, which is a heuristic algorithm imitating the musicians' structure for finding the best harmony, is widely used for solving the complex problems that cannot be solved by old methods. It has several advantages over previous optimization methods. It applies the last absolute mathematical features such as differentiability, continuity, and convexity [30]. According to the definition presented by Geem et al. [31], the HS algorithm is based on the minimum mathematical requirements and begins from probable random search; therefore, it does not require much secondary information. The vector introduces the final solution with regard to all the resulted vectors.

In HS algorithm, the musician looks for the best harmony that has been arranged aesthetically. Accordingly, the optimizer algorithms look for the best status with regard to the objective function. Each musician is associated with the decision variable, and the musical instruments' beats are sorted based on the importance of the decision variable. The musical harmony at a certain time is associated with the leader vector in a certain repetition. The hearer's enjoyment is the final objective (output of the harmony). Furthermore, just like the stepwise improvement of the musical harmony, the solution vector in the algorithm moves toward the optimal solution in each repetition [32].

Each musician has three options: (1) playing each pitch based on his own memory, (2) playing something similar to the given music, and (3) playing a new or random note. These explanations are generally expressed by the following formula [33]:

$$x_{new} = x_{old} + b_p \times (2rand - 1) \tag{17}$$

$$x(i) = x_{min}(i) + (x_{max}(i) - x_{min}(i)) \times rand \tag{18}$$

Where, x_{new} is the new solution after a certain beat, x_{old} is the solution from memory of harmony, $rand \in [0,1]$, b_p is the bandwidth vector, i is equal to 3, and $x_{min}(i)$ and $x_{max}(i)$ are the minimum and maximum values of i, respectively.

3. Implementing and executing the model

3.1 Preparing data

To prepare the data, the entire data were divided into two groups, namely training data (80%) and test data (20%). The input data, including inflow, reservoir water level, sluice gate outflow, intake flow rate, dam total outflow were used to predict the piezometric water level. It should be noted that in order to challenge the models in the previous data unavailability conditions, simulation was performed based on merely the data of each month; since, in case of desirable evaluation of the models, it would be possible to use them for any time period regardless of the physical performance and historical data of the dam's piezometers and merely based on the input data of that month.

3.2 Evaluating model's performance

In the present study, in order for evaluating the performance of the used models, several statistical indices, including MSE (mean square error), MAE (mean absolute error), and RMSE (root mean square error), and correlation coefficient (R) were used.

$$R = \frac{\sum_{i=1}^{N_O}(y_i - \bar{y})(m_i - \bar{m})}{\sqrt{\sum_{i=1}^{N_O}(y_i - \bar{y})^2 \sum_{i=1}^{N_O}(m_i - m)^2}} \tag{19}$$

$$MSE = \frac{1}{N_O}\sum_{i=1}^{N_O}(y_i - m_i)^2 \tag{20}$$

$$\mathrm{MAE} = \frac{1}{\mathrm{N_O}}\sum_{\mathrm{i=1}}^{\mathrm{N_O}}|\mathrm{y_i} - \mathrm{m_i}| \tag{21}$$

$$\mathrm{RMSE} = \sqrt{\frac{1}{\mathrm{N}}\sum_{\mathrm{i=1}}^{\mathrm{N_O}}(\mathrm{y_i} - \mathrm{m_i})^2} \tag{22}$$

where, y_i and m_i represent the network's output and measured data for i elements, respectively, and $\bar{y}$ and $\bar{m}$ represent the mean of parameters, and N_O indicates the number of them.

3.3 Setting up the models

In the present study, in order to predict the water level in piezometers 20, 28, and 30, the 3-layer neural network, regression decision tree, classification decision tree, and multivariate linear regression were used. Precision of any model is directly dependent on the input parameters; therefore, the input parameters included the monthly gathered data, including: evaporation, inflow, reservoir water level, sluice gate outflow, outflow, dam total outflow, and read water level of piezometers. The training data were considered as the basis of modelling for all the models. In order for modelling using neural networks, several neural networks with different architectures were taken into consideration. By considering different numbers of neurons in the network, the best state of the network was identified. Finally, by considering three neurons in the middle layer, the intended neural network was built, and performance of different transmission functions was compared. The neural network's parameters (weights and biases) were optimized using LM, PSO and HS algorithms. By initiating the weights and biases, the final values of these coefficients were extracted using the above-mentioned algorithms, and then these extracted values were used for modelling the neural network. The results obtained for different transmission function, considering three neurons in the middle layer, were evaluated so that these methods can be compared in the same conditions. In order for modelling via classification and regression decision trees, the intended models were constructed using the training data as the inputs; then, the performance of these models was evaluated using the test data.

4. Results and discussion

Investigating the results obtained from modelling the ANNs shows that in terms of simulation all the three piezometers, the neural network with 5 neurons exhibited the best performance. However, performance of the transmission function in the hidden and output layers was different for each piezometer, the results of which are summarized in Table (3).

Table 3- Results of modelling ANN-LM in order to simulate water level variations of piezometers of Jiroft Dam

Piezometer	ANN-LM	Train				Test			
		MSE (m^2)	MAE (m)	RMSE (m)	R	MSE (m^2)	MAE (m)	RMSE (m)	R
20	Tansig-Tansig	2.593	1.227	1.610	0.987	7.321	1.805	2.706	0.967
	Tansig-Logsig	2.646	0.982	1.627	0.987	4.113	1.580	2.028	0.988
	Logsig-Tansig	**2.712**	**1.016**	**1.647**	**0.987**	**4.077**	**1.667**	**2.019**	**0.991**
	Logsig-Logsig	1.964	0.872	1.401	0.990	10.029	1.656	3.167	0.960
28	Tansig-Tansig	5.596	1.589	2.365	0.968	20.565	3.550	4.535	0.911
	Tansig-Logsig	3.695	1.372	1.922	0.979	21.132	3.492	4.597	0.918
	Logsig-Tansig	**3.251**	**1.151**	**1.803**	**0.982**	**16.542**	**3.040**	**4.067**	**0.921**
	Logsig-Logsig	4.579	1.466	2.139	0.974	19.887	3.336	4.459	0.897
30	Tansig-Tansig	1.010	0.711	1.005	0.983	7.4383	2.063	2.727	0.918
	Tansig-Logsig	0.956	0.730	0.978	0.984	7.009	1.970	2.647	0.921
	Logsig-Tansig	**1.046**	**0.746**	**1.023**	**0.982**	**6.780**	**2.035**	**2.604**	**0.935**
	Logsig-Logsig	1.129	0.792	1.063	0.981	7.863	2.051	2.804	0.922

For the piezometer 20, the transmission function log sigmoid for the hidden layer tan sigmoid for the output layer exhibited the best performance; however, for the piezometer 28, the transmission function of tan sigmoid for both hidden and output layers had the best performance. Besides, in the piezometer 30, again both hidden and output layers with transmission function tan sigmoid had the best solutions. Since the use of 3 neurons in the hidden layer in the neural network resulted in the best performance, in the combination of the neural network with PSO and HS algorithm, 3 neurons were used in the hidden layer as well, the results of which are presented in Tables (4) and (5). Here, again the transmission functions of the hidden and output layers were different for each piezometer. In the neural network-PSO algorithm combination, piezometer 20 with transmission function of tan sigmoid for the hidden layer and log sigmoid for the output layer, piezometer 28 with log sigmoid transmission function for both hidden and output layers, and piezometer 30 with tan sigmoid transmission function for both layers exhibited the best performance. Moreover, in the combination of the neural network with HS algorithm, piezometer 20 with transmission function of tan sigmoid in the hidden layer and log sigmoid in the output layer, piezometer 28 with tan sigmoid transmission function for both hidden an output layers, and piezometer 30 transmission function of log sigmoid for the hidden layer and tan sigmoid for the output layer had the best solutions.

Table 4- Results of combining ANN-PSO in order to simulate water level variations of piezometers of Jiroft Dam

Piezometer	ANN-PSO	Train				Test			
		MSE (m^2)	MAE (m)	RMSE (m)	R	MSE (m^2)	MAE (m)	RMSE (m)	R
20	Tansig-Tansig	4.926	1.567	2.219	0.976	3.614	1.494	1.901	0.991
	Tansig-Logsig	**4.621**	**1.300**	**2.149**	**0.977**	**2.533**	**1.194**	**1.592**	**0.990**
	Logsig-Tansig	9.422	2.275	3.069	0.953	8.796	2.355	2.966	0.974
	Logsig-Logsig	4.739	1.457	2.177	0.977	3.965	1.477	1.991	0.992
28	Tansig-Tansig	4.599	1.421	2.145	0.974	13.455	2.898	3.668	0.938
	Tansig-Logsig	4.721	1.473	2.173	0.973	16.013	3.105	4.002	0.913
	Logsig-Tansig	5.701	1.656	2.387	0.968	14.379	3.090	3.792	0.930
	Logsig-Logsig	**5.611**	**1.511**	**2.369**	**0.968**	**11.549**	**2.736**	**3.398**	**0.945**
30	**Tansig-Tansig**	**3.475**	**1.424**	**1.864**	**0.956**	**3.253**	**1.374**	**1.803**	**0.948**
	Tansig-Logsig	3.505	1.486	1.872	0.943	3.626	1.432	1.904	0.942
	Logsig-Tansig	3.043	1.389	1.745	0.949	3.412	1.444	1.847	0.945
	Logsig-Logsig	2.922	1.361	1.709	0.952	3.329	1.386	1.824	0.948

Table 5- Results of combining ANN-HS in order to simulate water level variations of piezometers of Jiroft Dam

Piezometer	ANN-HS	Train				Test			
		MSE (m^2)	MAE (m)	RMSE (m)	R	MSE (m^2)	MAE (m)	RMSE (m)	R
20	Tansig-Tansig	8.997	2.212	2.999	0.955	7.928	2.297	2.815	0.965
	Tansig-Logsig	**12.459**	**2.230**	**3.529**	**0.946**	**4.479**	**1.599**	**2.116**	**0.988**
	Logsig-Tansig	16.502	2.767	4.062	0.933	5.909	1.929	2.431	0.975
	Logsig-Logsig	9.584	2.272	3.095	0.953	5.171	1.833	2.274	0.981
28	**Tansig-Tansig**	**6.051**	**1.709**	**2.459**	**0.967**	**11.399**	**2.465**	**3.376**	**0.933**
	Tansig-Logsig	4.731	1.513	2.175	0.974	14.659	3.044	3.829	0.934
	Logsig-Tansig	6.839	1.905	2.615	0.962	12.510	2.749	3.537	0.931
	Logsig-Logsig	7.794	1.948	2.792	0.958	16.840	3.370	4.104	0.927
30	Tansig-Tansig	2.593	1.226	1.610	0.960	5.381	1.689	2.319	0.919
	Tansig-Logsig	2.118	1.195	1.455	0.965	3.638	1.572	1.907	0.949
	Logsig-Tansig	**3.311**	**1.369**	**1.819**	**0.951**	**3.107**	**1.385**	**1.763**	**0.949**
	Logsig-Logsig	2.754	1.181	1.659	0.956	5.010	1.833	2.238	0.932

Based on the results obtained from the two classification and regression decision trees, it was

concluded that the regression decision tree had the best performance for all three piezometers (Table 6).

The results obtained from all methods are summarized in Table (6). The results shown for all methods calculated statistical parameters are at the suitable level, which implies that all soft computing technics predict water levels with high accuracy.

Table 6- Comparing the performance of all the applied methods used in this study

Piezometer	MODEL	Train				Test			
		MSE (m^2)	MAE (m)	RMSE (m)	R	MSE(m^2)	MAE (m)	RMSE (m)	R
20	**ANN-PSO**	**4.621**	**1.300**	**2.149**	**0.977**	**2.533**	**1.194**	**1.592**	**0.990**
	ANN-HS	12.459	2.230	3.529	0.946	4.479	1.599	2.116	0.988
	ANN-LM	2.712	1.016	1.647	0.987	4.077	1.667	2.019	0.991
	CDT	72.471	4.464	8.513	0.736	94.884	5.993	9.740	0.577
	RDT	4.725	0.887	2.173	0.976	13.987	1.767	3.739	0.948
	MLR	25.145	4.024	5.014	0.869	22.898	3.652	4.785	0.898
28	ANN-PSO	5.611	1.511	2.369	0.968	11.549	2.736	3.398	0.945
	ANN-HS	**6.051**	**1.709**	**2.459**	**0.967**	**11.399**	**2.465**	**3.376**	**0.933**
	ANN-LM	3.251	1.151	1.803	0.982	16.542	3.040	4.067	0.921
	CDT	22.438	2.753	4.736	0.908	41.285	4.842	6.425	0.784
	RDT	2.049	0.913	1.431	0.988	16.973	2.353	4.119	0.903
	MLR	12.372	2.946	3.517	0.928	19.802	3.801	4.449	0.884
30	ANN-PSO	2.922	1.361	1.709	0.952	3.329	1.386	1.803	0.948
	ANN-HS	**3.311**	**1.369**	**1.819**	**0.951**	**3.107**	**1.385**	**1.763**	**0.949**
	ANN-LM	1.046	0.746	1.023	0.982	6.780	2.035	2.604	0.935
	CDT	11.502	2.128	3.391	0.847	13.856	2.727	3.722	0.799
	RDT	0.475	0.417	0.689	0.992	3.345	1.173	1.829	0.940
	MLR	**2.834**	**1.336**	**1.683**	**0.952**	**3.067**	**1.450**	**1.751**	**0.945**

The obtained results indicate that for piezometer 20, the best performance was related to the ANN-PSO method, while piezometer 28 and 30 exhibited their best performance with ANN-HS and MLR methods, respectively.

In order to achieve a better understanding of the findings derived from the methods used in the present study, the obtained results are represented as dispersion diagrams for piezometers 20, 28, and 30 in Figures (6) to (8).

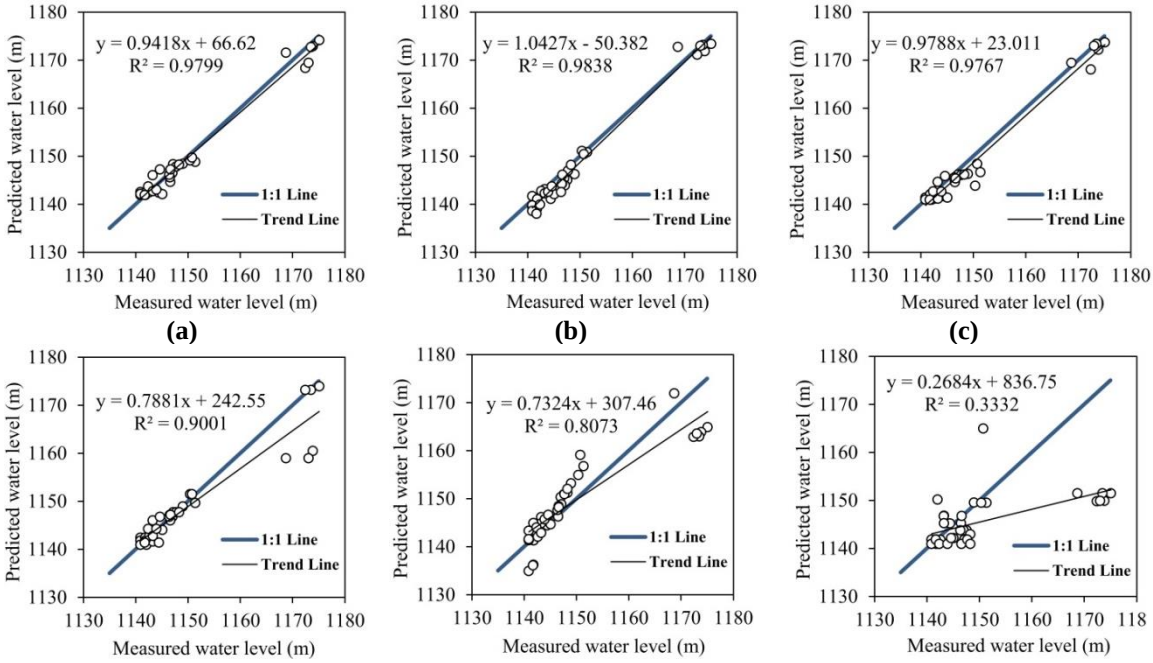

Figure 6. Results obtained from data-driven models in test stage for simulating piezometer 20 level variations; (a) ANN-PSO, (b) ANN-LM, (c) ANN-HS, (d) RDT, (e) MLR, (f) CDT

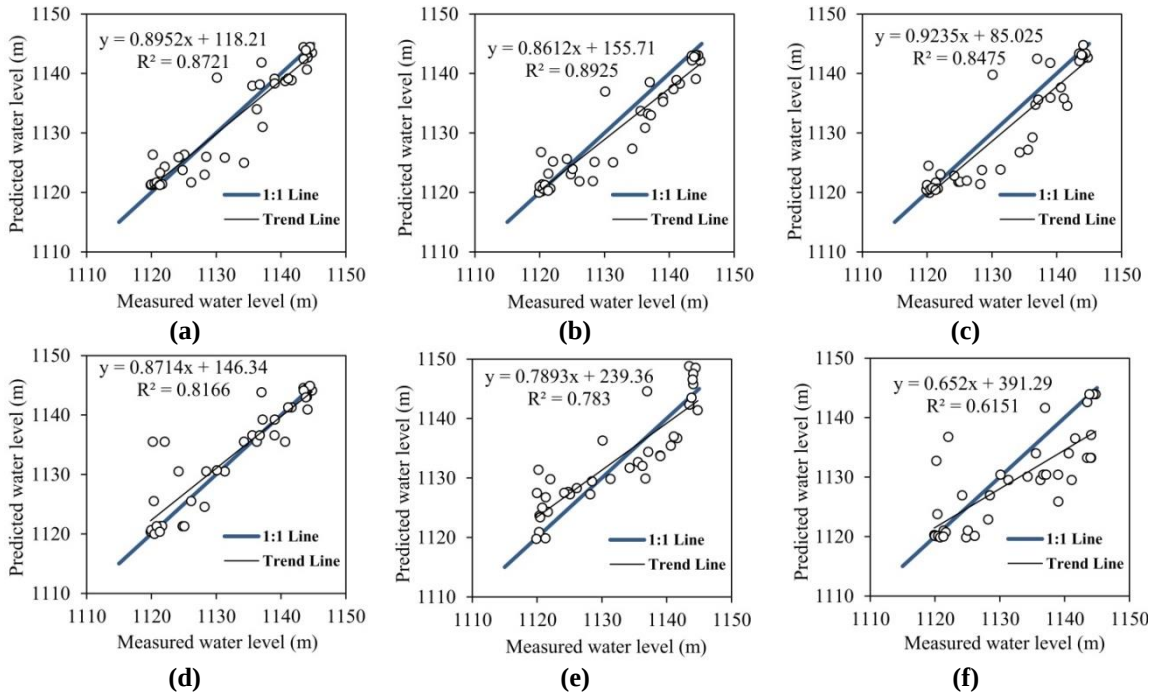

Figure 7- Results obtained from data-driven models in test stage for simulating piezometer 28 level variations; (a) ANN-HS, (b) ANN-PSO, (c) ANN-LM, (d) RDT, (e) MLR, (f) CDT

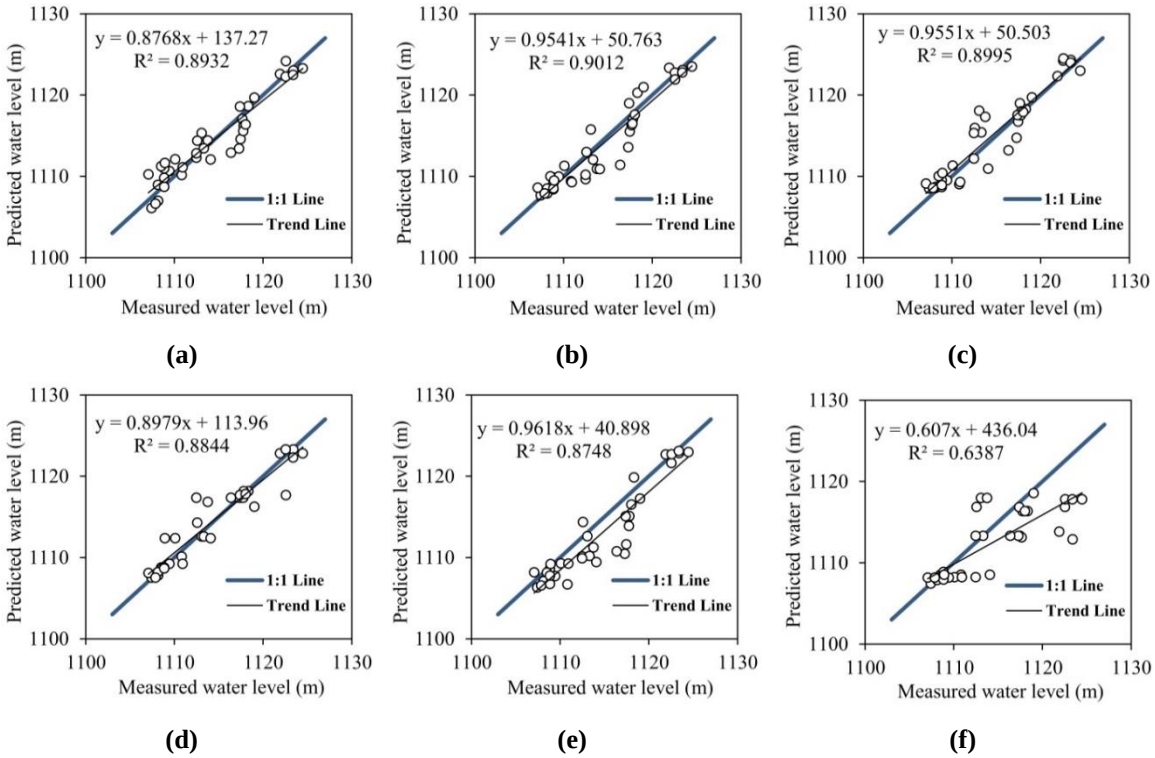

Figure 8. Results obtained from data-driven models in test stage for simulating piezometer 30 level variations; (a) MLR, (b) ANN-HS, (c) ANN-PSO, (d) RDT, (e) ANN-LM, (f) CDT

For piezometer 20, the best performance was obtained by combination ANN-PSO algorithm (considering RMSE criterion), while piezometer 28 exhibited its best performance in combination of ANN-HS algorithm. Besides, piezometer 30 showed its best performance by applying MLR method.

The Man-Whitney test can be used to investigate two groups' dependence or independence from the observed data. The initial hypothesis (H0) is that the two groups of data are equal, and the hypothesis-1 is that the average of the two groups of data are not statistically equal at a certain confidence level. The correct hypothesis can be determined by calculating the p-value at the given confidence level (α); so that, if the p-value is smaller than α, the H0 (equality of the two groups) will be rejected, and otherwise it will be accepted. In the present study, in order to answer the question that whether or not different soft computing methods used in the study have statistically significant differences, it was attempted to statistically investigate the case and perform the Man-Whitney test, the results of which are provided in Table (7).

Table 7- Statistical investigation of results obtained via Man-Whitney method

Piezometer	Model	p-value	Significantly different (95%)	Significantly different (99%)
20	Observed vs. ANN-LM	0.142	NO	NO
	Observed vs. ANN-HS	0.156	NO	NO
	Observed vs. ANN-PSO	0.872	NO	NO
	Observed vs. CDT	0.136	NO	NO
	Observed vs. RDT	0.979	NO	NO
	Observed vs. MLR	0.433	NO	NO
28	Observed vs. ANN-LM	0.483	NO	NO
	Observed vs. ANN-HS	0.921	NO	NO
	Observed vs. ANN-PSO	0.491	NO	NO
	Observed vs. CDT	0.135	NO	NO
	Observed vs. RDT	0.815	NO	NO
	Observed vs. MLR	0.659	NO	NO
30	Observed vs. ANN-LM	0.123	NO	NO
	Observed vs. ANN-HS	0.736	NO	NO
	Observed vs. ANN-PSO	0.533	NO	NO
	Observed vs. CDT	0.106	NO	NO
	Observed vs. RDT	0.921	NO	NO
	Observed vs. MLR	0.831	NO	NO

In Table (7), the results of the data driven models obtained by various methods were evaluated using Man-Whitney test. The results in Table (7) indicate that in all the models used in this study there was no significant difference between the modelling methods.

In this study, the hydraulics of governing equations for modelling the piezometric are actually captured by the black-box nature of the ANN models by adjusting synaptic weights in their structure. It is highly recommended to compare the results of numerical/mathematical methods for predicting the piezometric with the soft computing models. However, due to the limitation of having precise databases (such as hydraulic conductivity coefficient in the body of dam/foundation) for setting up numerical/mathematical, this could not be achieved in this study.

4. Conclusion

Soft computing is of special importance for solving the nonlinear problems. In this regard, the ANNs as well as their combination with meta-heuristic algorithms are highly regarded in solving the engineering problems. These networks are indeed powerful tools for optimizing the learning and generalizing the training samples; besides, they are among the most important soft computing sub-branches of the decision trees, which are commonly capable to predict and classify the quantitative and qualitative data and are widely used for solving the hydraulic and non-hydraulic problems.

Moreover, they are among the major effective parameters in dams' stability as well as its

relevant problems; therefore, dam seepage monitoring and also dam surveillance are of special importance for the safety of the dam. On this basis, the present study attempted to investigate the prediction of water level of piezometers of double-curvature arch dam using feed-forward multi-layer artificial neural network (FNN) with Levenberg-Marquardt optimization algorithm as well as PSO and HS algorithms along with classification and regression decision trees and multivariate linear regression model. Despite the appropriate performance of the methods used in simulating the piezometric water level variations, analysis of the statistical results of the used methods revealed the superiority of none of the method over the other ones.

References

1. Rankovic, V. Novakovic, A. Grujovic, N. Divac, D. & Milivojevic, N. 2014 Predicting piezometric water level in dam via artificial neural network. Neural Computing & Applications 24 (5), 1115-1121.
2. Li, M. C. Guo, X. Y. Shi, J. & Zhu, Z. B. 2015 Seepage and stress of anti- seepage structures constructed with different concrete materials in an RCC gravity dam.Water Science and Engineering 8 (4), 326-334.
3. Tan, X. Wang, X. Khoshnevisan, S. & Hou, X. 2017 Seepage analysis of earth dams considering spatial variability of hydraulic parameters. Engineering Geology 228, 260-269.
4. Xiang, Y. Fu, Y. S. Zhu, K. Yuan, H. & Fang, Z. Y. 2017 Seepage safety monitoring model of an earth rock dam under influence of high-impact typhoons on particle swarm optimization method. Water science and Engineering 10 (1), 70-77.
5. Zhou, C. B. Liu, W. Chen, Y. F. Hu, R. & Wei. K. 2015 Inverse modeling of leakage through a rockfill dam foundaction during its construction stage using transient flow model, neural network and genetic algorithm. Engineering Geology 187, 183-195.
6. Su, H. Tian, S. Kang, Y. Xie, W. & Chen, J.2017 Monitoring water seepage velocity in dikes using distributed optical fiber temperature sensors. Automation in Construction 76, 71-84.
7. Turkmen, S. Ozguler, E. Taga, H. & Karaogullarindan, T. 2002 Seepage problems in the karstic limestone foundation of the Kalecik Dam (south Turkey). Engineering Geology 63 (3-4), 247-257.
8. Tayfur, G. Swiatek, D. Wita, A. & Singh, V.P. 2005 Case study: finite element method and artificial neural network models for flow through Jeziorsko Earthfill Dam in Poland. Journal of Hydraulic Engineering 131 (6), 431-440.
9. Gholizadeh, S. & Seyedpoor, S. M. 2011 Shape optimization of arch dam by metaheuristics and neural networks for frequency constraints Science Iranica 18 (5), 1020-1027.

10. Stojanovic, B. Milivojevic, M. Milivojevic, N. & Antonijevic, D. 2016 A self-tuning system for dam behavior modeling based on evolving artificial neural network. Advances in Engineering Software 97, 85-95.

11. Nourani, V. Mousavi, S. Sadikoglu, F. & Singh, V. 2017 Experimental and AI-based numerical modeling of contaminant transport in porous media.Journal of Hydrology 205, 78-95.

12. Peymab Company. 1991 Report of Jiroft Dam Study.

13. Zounemat-Kermani, M., 2012 Hourly predictive Levenberg–Marquardt ANN and multi linear regression models for predicting of dew point temperature. Meteorology and Atmospheric Physics, 117(3-4),181-192.

14. Breiman, L. Friedman, J. H. Olshen, R. A. & Stone, C.J. 1984 Classification and regression tree. Chapman & Hall/CRC.

15. Swetapadma, A., & Yadav, A. (2017). A novel decision tree regression-based fault distance estimation scheme for transmission lines. IEEE Transactions on Power Delivery, 32(1), 234-245.

16. Lagacherie, P. & Holmes, S. 1997 Addressing geographical data errors in a classification tree for soil unit prediction. International Journal Geographical Information Science 11 (2),183-198.

17. Salazar, F. Toledo, M. A. Onate, E. & Suarez, B.2016 Interpretation of dam deformation and leakage with boosted regression tree. Engineering Structures 119, 230-251.

18. Nerini, D. Durbec, J. P. Mante, C. Garcia, F. & Ghattas, B. 2000 Forecasting physicochemical variables by a classification tree method application to the Berre Lagoon (South France). Acta Biotheoretica 48 (3-4), 181-196.

19. Paensuwan, N. Yokoyma, A. Verma, S.C. & Nakachi, Y. 2011 Application of Decision Tree Classification to the Probabilistic TTC Evaluation. Journal of International Council on Electrical Engineering 1 (3), 223-330

20. Seyedashraf, O. Rezaei, A. & Akhtari, A. A. 2017 Dam break flow solution using artificial neural network. Ocean Engineerig 142, 125-132.

21. Zounemat-Kermani, M., 2014 Principal component analysis (PCA) for estimating chlorophyll concentration using forward and generalized regression neural networks. Applied Artificial Intelligence, 28(1), pp.16-29.

22. Sapna, S. Tamilarasi, A. & Kumar, M. P. 2012 Backpropagation Learning Algorithm Based on Levenberg Marquardt Algorithm.Computer Science & Information Technology 07, 393-398.

23. Alsmadi, M. K. S. Omar, K. B. & Noah, S.A. 2009 Back Propagation Algorithm: The Best Algorithm among Multi-layer Perceptron Algorithm. International Journal of Computer Science and Network Security. 9,378-383.

24. Hamid, N. A. Nawi, N. M. GhaZali, R. & Salleh, M. N. M . 2011 Accelerating Learning Performance of Back Propagation Algorithm by Using Adaptive Gain Together with Adaptive Momentum and Adaptive Learning Rate on Classification Problems. International Journal of Software Engineering and its Applications 5, 31-44.

25. Zounemat-Kermani, M., Kisi, O. and Rajaee, T., 2013. Performance of radial basis and LM-feed forward artificial neural networks for predicting daily watershed runoff. Applied Soft Computing, 13(12), pp.4633-4644.

26. Kennedy, J. Eberhart, R. 1995 Particle swarm optimization. In: Proceedings of the 1995 IEEE I nternational Conference on Neural Networks, Perth, 4, 1942-1948.

27. Chau, K.W. 2006 Particle swarm optimization training algorighm for ANNs in stage prediction of Shing Mun River. Journal of Hydrology 329 (3-4), 363-367.

28. Gyanesh, D. Prasant, K. P. & Sasmita, K. P. 2014 Artificial Neural Network trained by particle swarm optimization for non-linear channel equalization. Expert Systems with Application 41 (7), 3491-3496.

29. Xiang, Y. Fu, Y. S. Zhu, K. Yuan, H. & Fang, Z. Y. 2017 Seepage safety monitoring model of an earth rock dam under influence of high-impact typhoons on particle swarm optimization method. Water science and Engineering 10 (1), 70-77.

30. Mun, S. & Cho, Y. H. 2012 Modified harmony search optimization for constrained design problems. Expert Systems Applications 39 (1), 419-423.

31. Geem, Z. W. Kim, J. & Loganathan, G. 2002 Harmony search optimization: Application to pipe network design. International Journal of Model Simulation 22, 125-133.

32. Yadav, P. Kumar, R. Panda, S. K. Chang, C.S. 2012 An Intelligent Tuned Harmony Search algorithm for optimization. Information science 196, 47-72.

33. Ruby, M. & Botez, R. M. 2016 Trajectory Optimization for vertical navigation using the Harmony Search algorithm. IFAC-PapersOnLine 49 (17), 11-16.